Experimental and Numerical Study on Aerodynamic Characteristics of Supersonic Biplane in Whole Speed Range

N. Kuratani, T. Ogawa*, M. Yonezawa*, H. Yamashita* and S. Obayashi**
**Institute of Fluid Science, Tohoku University*
2-1-1 Katahira, Aoba, Sendai, Miyagi 980-8577, Japan

Abstract
One of the critical technical issues on supersonic commercial transportation is the sonic boom at supersonic cruising that causes the large wave drag and the impulsive noise to the ground. Recently, the "supersonic biplane theory" has been proposed in order to reduce the sonic boom in supersonic cruising flight. However, some innovations and multidisciplinary design optimization are strongly required to improve the off-design performance. The wind tunnel testing in whole flight speed range has been conducted to investigate the flow characteristics and aerodynamic performance around the supersonic biplane and CFD analyses has assisted in understanding them comprehensively.

1. Introduction

Recently, commercial airplanes have been polarized into large and high-speed types, to satisfy various customer requirements all over the world. The former class with representatives such as the B747, can realize mass transit at low cost for intercontinental transport, moreover, it can provide superior comfort as in the case of the new A380. On the other hand, the latter type[1-2] proceeds to give first priority to economic efficiency, after the Concorde's retirement in 2003. Especially, in order to realize these high-speed airplanes, environmentally-driven technical issues have to be solved, e.g. noise around airports during take-off and/or landing, and sonic-boom in supersonic flight.

One of the critical technical issues of supersonic commercial transportation is the sonic boom at supersonic flight that causes large wave drag and impulsive noise to the ground. From the aspect of aerodynamics, the sonic boom induced by shock waves around the fuselage and the wing is inevitable during supersonic flight. Recently, the "supersonic biplane theory" has been proposed by Kusunose[3-4] to reduce the sonic boom. Just to note briefly, this concept utilizes the shock wave interference and cancellation between the wings of the Busemann biplane. Adolf Busemann proposed that sonic boom can be reduced by the interference between shock wave and expansion fan.[3-4] CFD (Computational Fluid Dynamics)[4-8] analyses have been conducted to verify this theory; moreover, CFD analyses and inverse design method[8] have been applied to the supersonic biplane conceptual design. Furthermore, CFD analyses can produce effective results and the flow phenomena can be captured comprehensively; however, they have to be validated by experimental results.[9-10]

This supersonic biplane has a remarkable advantage at supersonic cruising flight, however, not only the supersonic performance but also the transonic, subsonic and low-speed performance of supersonic biplane have to be understood and investigated to realize the supersonic commercial aircraft in the future. The purpose of this study is to investigate the fundamental flow characteristics and aerodynamic performance around supersonic biplane by wind tunnel testing and CFD analyses in the whole flight speed range.

2. Wind Tunnel Testing and Computational Methods

2.1 Supersonic and Transonic Wind Tunnel Testing

The supersonic biplane model is made of free-cutting stainless steel for a sharp leading-edge, as shown in Figure 1. This experimental model is used for both supersonic and transonic wind tunnel testing at the Institute of Space and Astronautical Science (ISAS), Japan Aerospace Exploration Agency (JAXA). The test section has 600 mm x 600 mm cross-sectional area. This two-dimensional model was made in order to investigate the flow characteristics between the wings of the biplane. The coordinate system utilized for the experiment and the CFD results is shown in Figure 1.

In order to compare with CFD analyses and theoretical studies,[3-7] the dimensions of this biplane model have been decided as follows: wing thickness ratio; t/c=0.05. Here, t is the biplane model thickness and c, is the chord length of the biplane. The dimensions of the biplane model are determined by the blockage ratio and the starting load in the supersonic wind tunnel facility. This experimental model has the following dimensions: c=80 mm, t=4 mm and wing span w=60 mm. The interplane distance at the biplane shoulder is G^*=32 mm and the distance at the leading edge is G=40 mm and G/c=0.5. This configuration of supersonic biplane enables the interference and cancellation of the shock waves between the wings of the biplane at a design Mach number M_∞=1.7, according to theoretical and Euler calculations.[3-7] The aspect ratio of AR=0.75 for this biplane model is smaller than the standard one. The standard aspect ratio is more than 1.5 to avoid the interference by Mach cones from both wing tips on the surface of the biplane. The previous CFD analyses[5, 7] were usually conducted under the aspect ratio AR=4.0. However, the surface area of this biplane model must be smaller to reduce the starting load in this wind tunnel testing. As a result, the wing span of biplane was decreased to AR=0.75 and w=60 mm.

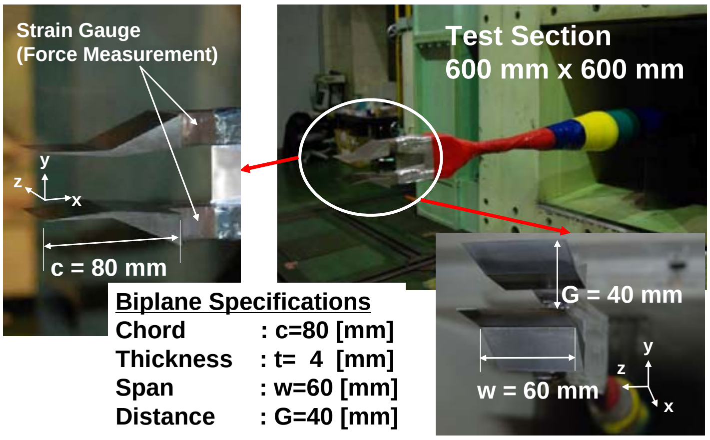

Figure 1: Overview of supersonic biplane model in test section for supersonic and transonic wind tunnel facilities

2.2 Low-speed Wind Tunnel Testing

Low-speed experiments were conducted in the low turbulence wind tunnel facility at the Institute of Fluid Science, Tohoku University. The two-dimensional experimental model is shown in Figure 2. This model is made of free-cutting brass, and the acrylic end plate is in diameter ϕ=200 mm and attached with the biplane model to keep the distance between the wings of the biplane. The biplane specifications are as follows: chord length c=100 mm, wing thickness t=5 mm (t/c=0.05), wing span w=150 mm and wing distance G=50 mm (G/c=0.5). These model specifications are same as the supersonic and transonic wind tunnel experimental model.[5-8]

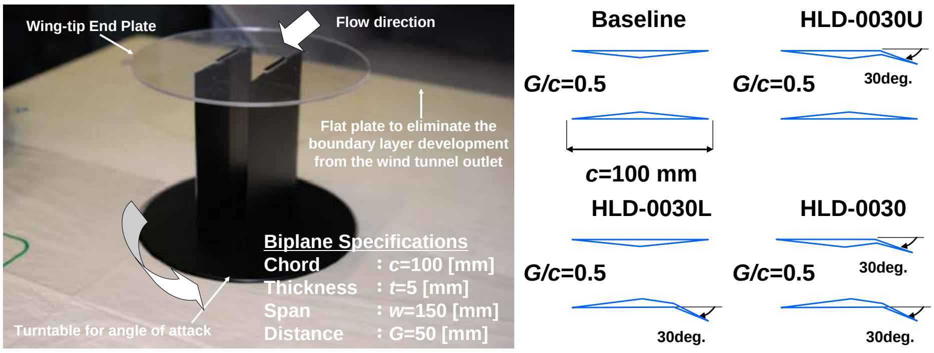

Figure 2: Supersonic biplane model for low-speed wind tunnel facility and biplane models with and without high-lift-devices

Moreover, the high-lift-devices are attached with the baseline biplane model to improve the low-speed aerodynamic performance such as the lift coefficient, C_L. These experimental models are illustrated in Figure 2. These high-lift-devices are served as the trailing edge flaps. And the flap angle is fixed to 30 deg. Here, HLD-0030U indicates that the biplane has a trailing edge flap of upper wing, HLD-0030L has a trailing edge flap of lower wing and HLD-0030 has both trailing edge flaps of upper and lower wings, as shown in Figure 2.

The aerodynamic performance such as lift, drag and pitching moment can be measured by three-force balance (Nissho-Electric-Works: LMC-3501-50NS) with the change in free-stream velocity U_∞ and angle of attack α, respectively. These measurement data are captured by LabVIEW (National Instruments) in personal computer during wind tunnel operation. The measurement duration is 20 sec and sampling rate 1 kHz.

Angle of attack can be changed by the turntable downside of the experimental model. Moreover the flat plate is installed upstream of the biplane model to eliminate the boundary layer from the outlet of the wind tunnel. And the measurement devices, installed downside of the biplane model, are covered with the fairing to eliminate the inlet air.

2.3 Computational Methods

2.3.1 Computational Method for Supersonic and Transonic Condition

A three-dimensional unstructured flow solver named TAS code (Tohoku University Aerodynamic Simulation code) [12-19] using three dimensional unstructured grid is performed to investigate the supersonic and transonic flow around the biplane. Navier-Stokes equations are solved by a finite-volume cell-vertex scheme. A hybrid volume grid composed of tetrahedrons, prisms, and pyramids is used for Navier-Stokes computations. The numerical flux is computed using the approximate Riemann solver of Harten-Lax-van Leer-Einfeldt-Wada (HLLEW).[21] The second order spatial accuracy is realized by a linear reconstruction of the primitive gas dynamic variables with Venkatakrishnan's limiter. The lower/upper symmetric Gauss-Seidel (LU-SGS) implicit method for unstructured mesh[22] is used for the time integration. The one-equation turbulence model[23] by Spalart-Allmaras is introduced to treat the turbulent boundary layers and solve the Navier-Stokes equations.

2.3.2 Computational Method for Low-speed Condition

A three-dimensional unstructured flow solver named TAS code[12-19] is also employed to simulate the low-speed flow fields in this study. The pseudo two-dimensional computation can be performed by the stretched three-dimensional grid in y-direction at constant. Three-dimensional Navier-Stokes equations are treated in this solver. The wing configuration data is generated by CATIA (DASSULT SYSTEMS). The computational grid around the supersonic biplane is generated by Edge Editor, which is unstructured grid generator[11]. The reasons why the unstructured grid has been adapted are as follows: superior in the adaptive configuration and to allow the complicated wing configuration with some high-lift-devices such as flap and slat in the near future.

CFD analyses are performed to investigate the flow filed around the two- and three-dimensional biplane models in low-speed range. Three-dimensional CFD analysis simulates the experimental study with an end plate and the flat plate to eliminate the boundary layer as shown in Figure 2. The total computational grid is 0.10 million in the case of two-dimensional model (2D-CFD) and 3.53 million in the case of three-dimensional model (3D-CFD)

The pre-processing is introduced to this TAS code for compressible flow analysis to deal with the incompressible flow such as low-speed range.[20] The differences between the existing TAS code and current one are numerical flux computation by pre-processing[21-22], the change in the lower/upper symmetric Gauss-Seidel (LU-SGS) implicit method for unstructured mesh[23] and SST k-ω turbulence model.[19] The reference speed U_{ref} as pseudo sonic speed is calculated to stabilize the convergence performance.[20] The turbulence intensity T_u is 1 % in free-stream for SST k-ω turbulence model and there is assumed to be fully turbulent flow. The free-stream velocity U_∞ is changed from 10 to 30 m/s and angle of attack α is changed from 0 to 25 deg. The Reynolds number, Re is setup from 2.46×10^4 to 1.73×10^5. The characteristic length is the chord length, c=100 mm.

3. Results and Discussion

3.1 Supersonic Wind Tunnel Testing

3.1.1 Design Mach number and Starting Characteristics

Wind tunnel testing at a design Mach number, M_∞=1.7, is performed in supersonic wind tunnel facility to achieve the shock wave interaction and cancellation between the wings of the biplane. This configuration of the biplane, G^*/G=0.8, can not be satisfied with Kantrowitz-Donaldson criterion[24-27] at a design Mach number [9-10]. Consequently, this experimental biplane model is predicted to not start, that is, shock wave interaction and cancellation between the wings of the supersonic biplane could not be achieved. However, the Schlieren photographs shows the shock wave interaction and cancellation between the wings of the supersonic biplane at M_∞=1.7 as shown in Figure 3. The shock waves from the leading edge of the wings reached the apex of the biplane, and the expansion fans were propagated. Especially, the expansion fans from the apex of the biplane were darkened due to the higher pressure gradient.

Why was the shock wave interaction and cancellation between the wings of supersonic biplane achieved at the design Mach number? It is believed that the higher pressure between the wings due to the shock waves propagating from the leading edge of the wings caused the spill out of the biplane. The static pressure outside of the biplane is lower than that between the wings due to the free-stream supersonic flow. Such a three-dimensional effect results in the avoidance of the unstart characteristics. To analyze this three-dimensional effect, the model is rotated by 90 degrees for the upside view of the model as shown in Figure 3. This photograph shows that the Mach waves propagate downstream from the leading edge of the biplane. Downstream of the Mach waves, the shock/boundary interaction was visualized on the surface of the biplane. In addition, the dark area around the middle of the biplane shows the interaction with the detached shock and compression waves upstream of the ramp for supporting system.

The pressure coefficient, C_p contour maps by CFD analyses with *AR=0.75* are shown in Figure 3 to investigate the shock interaction and cancellation, and the three-dimensional effect around the biplane, comparatively with the Schlieren photographs. The side view in the *x-y* plane shows the shock wave interaction and cancellation between the wings, and the weaker waves around the wing tip. Also, the upside-view in the *x-z* plane allows the visualization of the three-dimensional flow to the outside of the biplane. This biplane configuration plays a role as a supersonic diffuser and nozzle at the design Mach number. As shown in Figure 3, the internal flow through the biplane is accelerated by this configuration at the exit of the biplane. These Schlieren photographs and CFD analyses are in good agreement with each other qualitatively. Also, these CFD analyses can help us better understand the flow phenomena around the biplane.

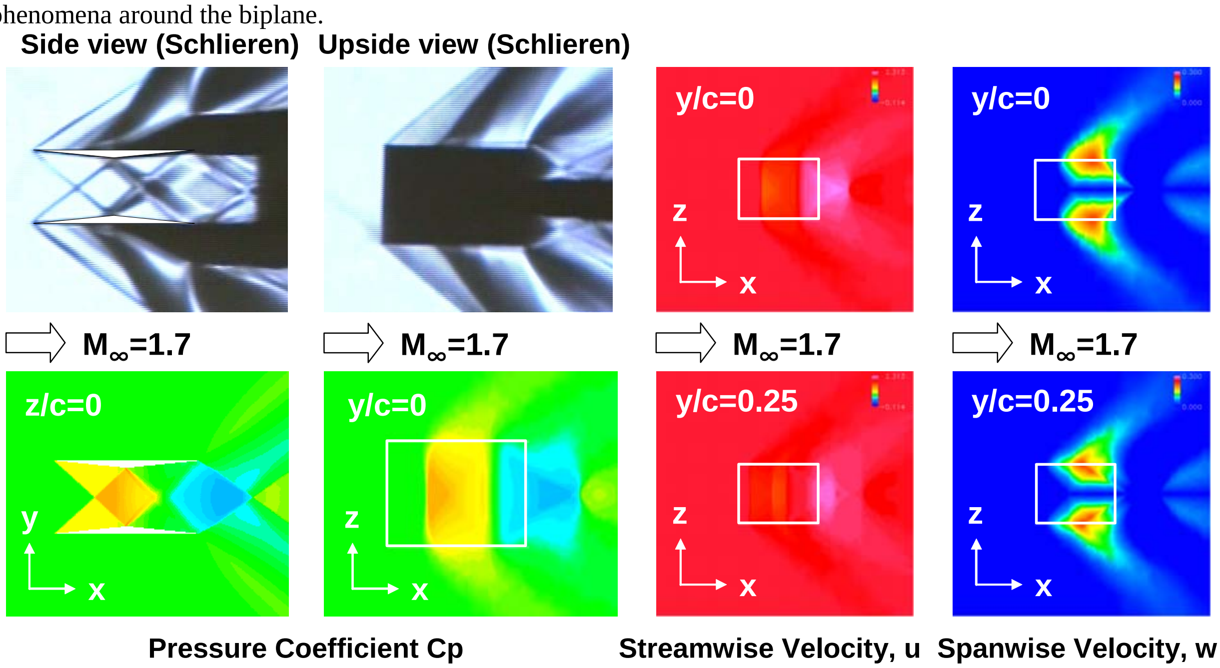

Figure 3: Shock wave interaction and cancellation between the wings of supersonic biplane by Schlieren photographs and C_p and velocity contour maps by CFD analyses at design Mach number, M_∞=1.7

3.1.2 Off-design Mach number

In addition, the wind tunnel testing at off-design Mach numbers were conducted in order to find out at which Mach number the unstart characteristics occurred. Experiments at M_∞=1.5 to 2.3 were conducted in the supersonic wind tunnel testing facility. The Schlieren photographs and C_p contour maps by CFD analysis are shown in Figure 4 under M_∞=1.5, 1.7, 1.9 and 2.1. The shock angle at the leading edge of the biplane is gradually larger at a Mach number smaller than the design Mach number, M_∞=1.7. These shock wave can not reach the apex of the biplane at M_∞= 1.5 as shown in Figure 4. The shock waves in the biplane, the shock waves reflected by the opposite side of the wing, and the expansion fans from the apex of the biplane interfere, and result in the complicated flow. Especially at M_∞ =1.5 the rearward biplane acts as a supersonic nozzle that accelerates the flow downstream of the apex of the biplane.

On the other hand, the shock angle is gradually smaller at a Mach number more than M_∞= 1.7. Figure 4 shows that the shock waves can reach the rearward wing at M_∞= 1.9 and 2.1. The swallowing Mach number under this biplane configuration is M_∞=2.1 based on the Kantrowitz-Donaldson Criterion. It is clear that the supersonic biplane can always be started under more than the swallowing Mach number, as shown in Figure 4. In these case the rearward biplane performs as supersonic nozzle and the flow is accelerated to more than the inlet Mach number

Consequently, the supersonic biplane under *AR*=0.75 can be started under M_∞=1.5 to 2.3. The three-dimensional effects are emphasized to start the supersonic biplane without the wing tip in the case of smaller wing aspect ratio.

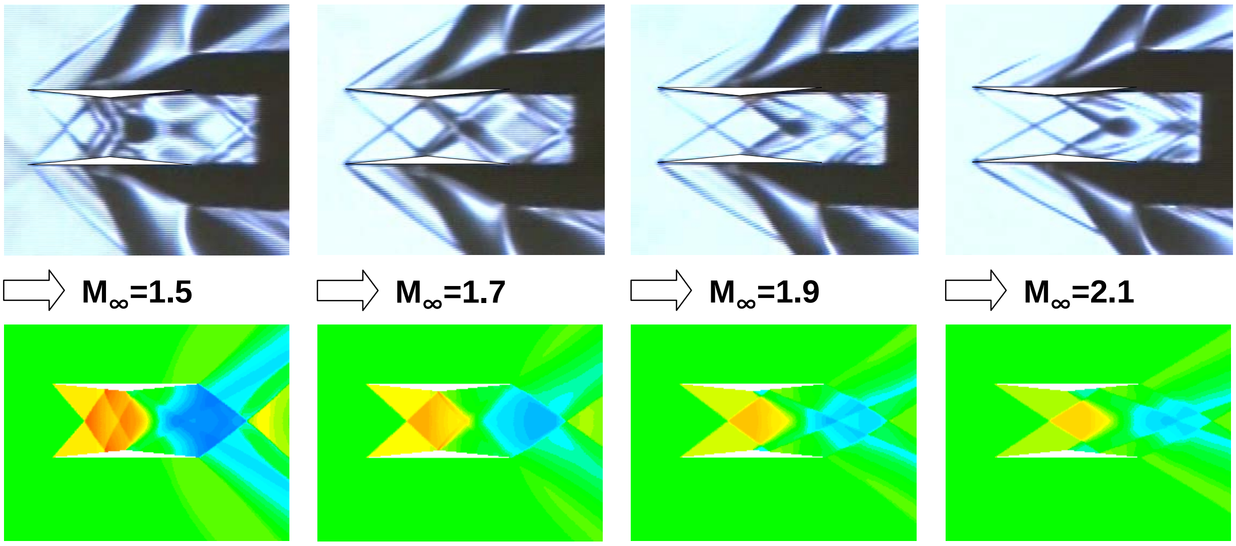

Figure 4: Schlieren photographs and C_p contour maps by CFD under off-design Mach numbers

3.2 Shock and Flow Patterns in Subsonic and Transonic flow

Schlieren flow visualization is introduced to visualize and investigate the flow characteristics around the supersonic biplane under the transonic flow condition M_∞=0.3 to 1.3. The Schlieren photographs under transonic condition in Mach number in 0.1 are shown in Figure 5. They were taken within Mach-sweep wind tunnel operation from 1.3 to 0.6 and 0.9 to 0.3. The model was rotated by 90 degrees for the upside view at M_∞=1.3 as shown in Figure 5.

There is a little change in density in the subsonic flow, M_∞<0.5, but there are gradually changes in the flow from the leading edge of the biplane and around the apex of the biplane M_∞>0.5. The forward supersonic biplane acts as the subsonic nozzle and accelerates the flow between the wings. There are remarkable contrast shown in Schlieren photographs at M_∞=0.7. This rearward supersonic biplane acts as the supersonic nozzle and accelerates the flow between the wings and there are the expansion waves around the trailing edge of the biplane.

From M_∞=0.8 to 0.9, the flow between the forward wings is accelerated by expansion fans in the remarkable contrast area. The obvious expansion fans between the wings indicates that the forward supersonic biplane acts as the supersonic diffuser and the rearward one does as the supersonic nozzle under M_∞=1.0 to 1.3. Especially, there is the detached shock wave upstream of the leading edge of biplane. And the second shock wave attaches at the visualization window and the there are the clear expansion waves around the ramp for supporting system.

At M_∞=1.2, the attached shock wave at the leading edge of biplane would cause the large drag and downstream of this shock wave there is the accelerated flow by the forward and rearward biplane as subsonic and supersonic nozzle. At M_∞=1.3, both side and upside views show that there are the shock waves from the leading edge of the biplane. These shock waves can turn the flow between the wings and there is the three-dimensional flow to the outside of the biplane as mentioned.

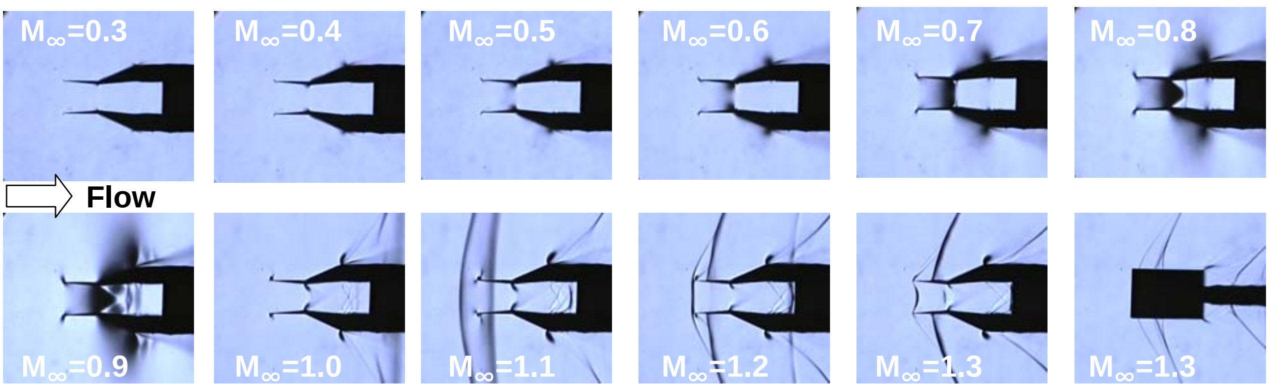

Figure 5: Schlieren photographs of transonic and subsonic flow fields around supersonic biplane under off-design Mach numbers (M_∞=0.3 to 1.3)

3.3 Low-speed Wind Tunnel Testing

3.3.1 Low-speed aerodynamic performance of baseline biplane

The lift and drag coefficients, C_L and C_D, are shown in Figure 6 with angle of attack under the free-stream velocity, U_∞=10 to 30 m/s. These coefficients are independent of free-stream velocity. C_L has original-point symmetry and C_D has axial one in whole angle of attack range. These results show the similar characteristics of the standard airfoil. And the stall angle is almost same as 18 deg. And there is the discrepancy between the two-dimensional CFD analysis (2D-CFD) and experiment as shown in Figure 6 under U_∞=30 m/s at constant. Especially, C_L by 2D-CFD is much higher than the one by experiment, and it is overestimated. Meanwhile, three-dimensional CFD analysis (3D-CFD) is good agreement with the experiment until the stall angle. Although the biplane model is two-dimensional one, the endplate, the wing-root and the flat plate to eliminate the boundary layer induce three-dimensional flow around the biplane. These effects cannot be ignored to estimate the aerodynamic performance precisely.

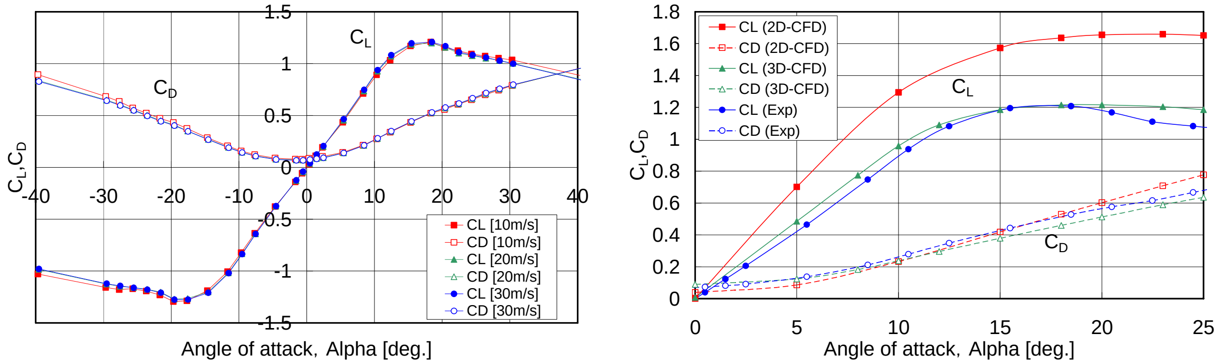

Figure 6: Lift and drag coefficients of supersonic biplane in low-speed range by wind tunnel testing (left figure) and that by wind tunnel testing, 2D- and 3D-CFD analyses under U_∞=30 m/s (right figure)

3.3.2 Improvement in low-speed aerodynamic performance with high-lift-devices

The high-lift-devices such as the trailing edge flaps are installed with the baseline model to improve the low-speed aerodynamic performance, as shown in Figure 2.With angle of attack α, under U_∞=10 m/s at constant, the lift coefficients C_L and the lift-to-drag ratios L/D are shown in Figure 7. All cases with the trailing edge flap show the remarkable increase in C_L. Both the cases of HLD-0030 and HLD-0030L show the maximum C_L, but the stall angles are decreased. In the case of HLD-0030U, maximum C_L did not increase sufficiently, the stall angle decreases and is a minimum. The baseline biplane shows maximum L/D among them due to the minimum drag coefficient C_D, because the increase in the projected area by flap deployment causes the increase in C_D in the other cases.

These experimental data for biplane model with and without high-lift-devices are summarized in Table 1. As mentioned, the trailing edge flap can produce the increase in C_L and C_D, but in the case of HLD-0030U the effect of it cannot be sufficiently achieved. This is the reason why the upper wing of the biplane is stalled at the lowest angle of attack. And, stall angle in this case is smaller than the other cases. On the other hand, L/D_{max} of HLD-0030U is higher than that of HLD-0030 and HLD-0030L, due to the smaller drag coefficient at the lower angle of attack.

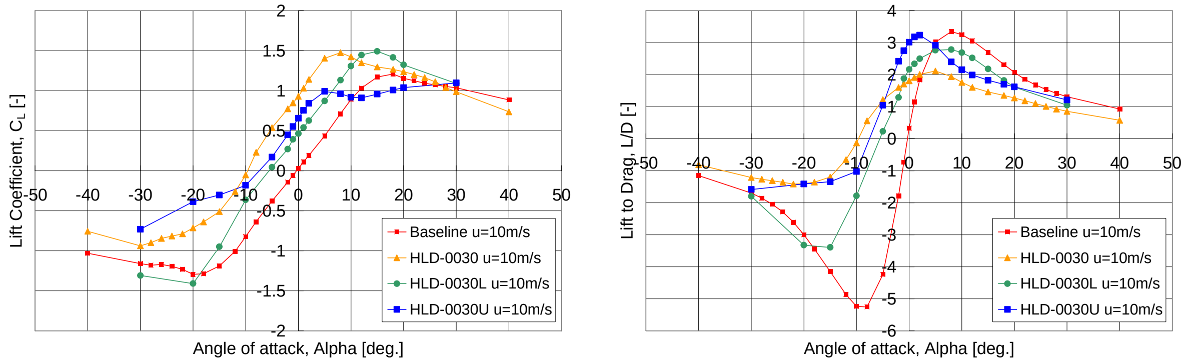

Figure7: Lift coefficient and Lift-to-Drag of supersonic biplane with and without the trailing edge flap in low-speed range by wind tunnel testing (U_∞=10 m/s)

Table 1: Low-speed aerodynamic characteristics of supersonic biplane with and without the trailing edge flap

Model	C_{Lmax}	α_{stall}	L/D_{max}	$\alpha_{L/Dmax}$
Baseline	1.20	18	3.34	8
HLD-0030U	0.99	5	3.24	2
HLD-0030L	1.49	15	2.78	8
HLD-0030	1.47	8	2.11	5

4. Conclusion and Future Works

The wind tunnel testing in supersonic, transonic and low-speed flow combined with CFD analyses was performed to investigate the flow characteristics and aerodynamic performance around the two-dimensional supersonic biplane model with and without high-lift-devices under whole flight speed range. The conclusions that can be drawn from this study are as follows:

1) Shock wave interaction and cancellation between the wings of the supersonic biplane were experimentally achieved at a design Mach number. The shock patterns and flow field around the supersonic biplane were qualitatively visualized and investigated by Schlieren photographs and CFD analyses not only at a design Mach number but also at off-design ones.
2) This two-dimensional biplane experimental model with AR=0.75 has a potential to cause the unstart characteristics based on Kantrowitz Donaldson criterion, however, the starting characteristics were experimentally demonstrated by the spill out flow outside the wings due to the pressure difference.
3) The supersonic biplane plays a role in being nozzle and/or diffuser, such as an intake-diffuser, based on the inlet flow condition in transonic and subsonic flow during Mach-sweep wind tunnel operation.
4) The fundamental low-speed aerodynamic performances C_L and C_D around baseline supersonic biplane are independent of the free-stream velocity by wind tunnel testing.
5) It was clarified that the aerodynamic performance was quantitatively affected by the three-dimensional flow around the wing root of baseline supersonic biplane, compared with two- and three-dimensional CFD analyses and wind tunnel testing.
6) The effects of the high-lift-devices such as a trailing edge flap to the increase in C_L and the decrease in stall angle were clarified. The trailing edge flap of lower wing affects the increase in C_L and the change in projected area by high-lift-device deployment and angle of attack have to be monitored in order to decrease C_D.

Concurrently executed with CFD analyses and experiments, these interdisciplinary data will hopefully assist in the effective conceptual design of supersonic biplane by multidisciplinary optimization design, MDO, and multi objective design exploration, MODE in the near future.

Acknowledgments

The authors would like to thank Dr. Tomoko Irikado and Mr. Kiyoshi Satoh of the Institute of Space and Astronautical Science (ISAS), the Japan Aerospace Exploration Agency (JAXA) for considerable supports for executing the supersonic and transonic wind tunnel testing. The authors also would like to thank Prof. Kawazoe, Dr. Matsuno at the Faculty of Engineering, Tottori University, for their considerable discussions and supports for Low-speed wind aerodynamic study. The authors also would like to thank Dr. Koji Shimoyama and Mr. Atsushi Toyoda at the Institute of Fluid Science, Tohoku University, for considerable supports for executing all the mentioned wind tunnel testing.

This study is supported by Grant-in-aid scientific research (No. 15206091), Ministry of Education, Culture, Sports, Science and Technology in Japan, "Silent Supersonic Transportation Workshop" of Aerodynamic Division Committee, The Japan Society for Aeronautical and Space Sciences, and 21st Century COE Program "International COE of Flow Dynamics", Institute of Fluid Science, Tohoku University. The authors would like to thank the Advanced Fluid Information Research Center in Institute of Fluid Science, Tohoku University, for the computational resources used in this study.

References

[1] Aerion Corp., http://www.aerioncorp.com/
[2] HISAC project, http://www.hisacproject.com/

[3] Kusunose, K., A New Concept in the Development of Boomless Supersonic Transport, *1st International Conference on Flow Dynamics*, pp.46-47, 2004.
[4] Kusunose, K., Matsushima, K., Goto, Y., Yamashita, H., Yonezawa, M., Maruyama, D., and Nakano, T., A Fundamental Study for the Development of Boomless Supersonic Transport Aircraft, *44th AIAA Aerospace Sciences Meeting and Exhibit*, AIAA 2006-0654, 2006.
[5] Yonezawa, M., Yamashita H., Obayashi, and S., Kusunose, K., Investigation of Supersonic Wing Shape Using Busemann Biplane Airfoil, *45th AIAA Aerospace Sciences Meeting and Exhibit*, AIAA-2007-0686, 2007.
[6] Yamashita, H., Yonezawa, M., Obayashi, and S., Kusunose, K, A Study of Busemann- Type Biplane for Avoiding Choked Flow, *45th AIAA Aerospace Sciences Meeting and Exhibit*, AIAA 2007-0688, 2007.
[7] Maruyama, D., Matsushima, K., Kusunose, K., and Nakahashi, K, Aerodynamic Design of Biplane Airfoils for Low Wave Drag Supersonic Flight, *24th AIAA Applied Aerodynamics Conference*, AIAA 2006-3323, 2006.
[8] Maruyama, D., Matsuzawa, T., Kusunose, K., Matsushima, K., and Nakahashi, K., Consideration at Off-Design Conditions of Supersonic Flows around Biplane Airfoils, *45th AIAA Aerospace Sciences Meeting and Exhibit*, AIAA 2007-0687, 2007.
[9] Furukawa, T., Kumagai, N., Oshiba, S., Ogawa, T., Saito, K., and Sasoh, A., Experimental and Theoretical Examinations on Shock Wave Phenomena for Silent Supersonic Biplane, *3rd International Symposium on Transdisciplinary Fluid Integration TFI-2006*, pp.55-56, 2006.
[10] Kuratani, N., Ogawa, T., Yamashita, H., Yonezawa, M., and Obayashi, S., Experimental and Computational Fluid Dynamics around Supersonic Biplane for Sonic-Boom Reduction, *13th AIAA/CEAS Aeroacoustics Conference*, AIAA 2007-3674, 2007.
[11] Ito, Y. and Nakahashi, K., Improvements in the Reliability and Quality of Unstructured Hybrid Mesh Generation, *International Journal for Numerical Methods in Fluids*, Vol. 45, Issue 1, pp. 79-108, 2004.
[12] Ito, Y., and Nakahashi, K., Direct Surface Triangulation Using Stereolithography (STL) Data, *38th AIAA Aerospace Sciences Meeting and Exhibit*, AIAA 2000-0924, 2000.
[13] Sharov, D., and Nakahashi, K., Hybrid Prismatic/Tetrahedral Grid Generation for Viscous Flow Applications, *27th AIAA Flow Dynamics Conference*, AIAA 96-2000, 1996.
[14] Ito, Y., and Nakahashi, K., Unstructured Mesh Generation for Viscous Flow Computations, *Proceedings of the 11th International Meshing Roundtable*, pp. 367–377, 2002.
[15] Toyoda, A., Misaka, T. and Obayashi, S., "Application of Correlation-Based Transition Prediction Method to JAXA High-Lift Configuration Model", *37th AIAA Fluid Dynamics Conference and Exhibit*, AIAA 2007-4286, 2007 (in print).
[16] Weiss, J. M., Maruszewski, J. P. and Smith, W. A., "Preconditioned Applied to Variable and Constant Density Flows," *AIAA Journal*, Vol. 33, No. 11, pp. 2050–2057, 1995.
[17] Mukai, J., Influences of Artificial Viscosity Terms on Unsteady Calculation of Low-Speed Flowfield, *37th Aerospace Numerical Simulation Symposium 2005*, *JAXA-SP-05-017*, pp.156-161, 2005, (in Japanese).
[18] Sharov, D. and Nakahashi, K., Low Speed Preconditioning and LU-SGS Scheme for 3-D Viscous Flow Computation on Unstructured Grids, *36th AIAA Aerospace Sciences Meeting and Exhibit*, AIAA 98-0614, 1998.
[19] Menter, F. R. Zonal two-equation k-ω turbulence model for aerodynamic flows, *23rd AIAA Fluid Dynamics, Plasmadynamics and Lasers Conference*, AA 93-2906, 1993
[20] Luos, H., Baum, J. D. and Lohner, R., "Extension of Harten-Lax-van Leer Scheme for Flows at All Speeds," *AIAA Journal*, Vol. 43, No. 6, pp. 1160–1166, 2005.
[21] Obayashi, S., and Guruswamy, G. P., "Convergence Acceleration of an Aeroelastic Navier-Stokes Solver," *AIAA Journal*, Vol. 33, No. 6, 1994, pp. 1134–1141.
[22] Sharov, D., and Nakahashi, K., "Reordering of Hybrid Unstructured Grids for Lower-Upper Symmetric Gauss-Seidel Computations," *AIAA Journal*, Vol. 36, No. 3, pp. 484–486., 1998
[23] Spalart, P., R., and Allmaras, S., R., "A One-Equation Turbulence Model for Aerodynamics Flows," *30th AIAA Aerospace Sciences Meeting and Exhibit*, AIAA Paper 92-0439, 1992.
[24] Van Wie, D., M., Kwok, F., T., and Walsh, R., F., "Starting Characteristics of Supersonic Inlet," *32nd AIAA/ASME/SAE/ASEE Joint Propulsion Conference*, AIAA 96-2914 ,1996.
[25] Van Wie, D., M., White, M., E., Waltrup, P., J., "Application of Computational Design Techniques in the Development of Scramjet Engines," *AIAA 19th Fluid Dynamics, Plasma Dynamics and Lasers Conference*, AIAA 87-1420, 1987.
[26] Van Wie, D., M., Molder, S., "Applications of Busemann Inlet Designs for Flight at Hypersonic Speeds," *AIAA Aerospace Design Conference*, AIAA 92-1210, 1992.
[27] Molder, S., Szpiro, E., J., "Busemann Inlet for Hypersonic Speeds," *Journal of Aircraft*, Vol.3, No.8, pp.1303-1304, 1996.

eucass

This page has been purposedly left blank